

# Effects of the injection direction of pilot fuel on combustion and emissions under two-stroke HPDI dual fuel marine engine-like conditions

Arash Nemati<sup>1\*</sup>, Jiun Cai Ong<sup>1</sup>, Jens Honore Walther<sup>1,2</sup>

1 Department of Mechanical Engineering, Technical University of Denmark, 2800 Kgs. Lyngby, Denmark

2 Computational Science and Engineering Laboratory, ETH Zürich, CH-8092 Zürich, Switzerland

## ABSTRACT

A numerical study on effects of the injection direction of the pilot diesel fuel on combustion and emissions under two-stroke dual-fuel marine engine-like conditions is presented in this paper. It is found that the injection direction of the pilot fuel has significant effects on the methane start of combustion as well as flame propagation direction which leads to different heat transfer trends to combustion chamber walls and flame-wall interaction. Furthermore, the injection direction of the pilot fuel changes the methane combustion intensity which leads to different trends for emission formation.

**Keywords:** Marine engine, dual fuel, CFD, high pressure direct injection, injection direction

## 1. INTRODUCTION

Large two-stroke marine engines are the main source of propulsion in the shipping industry. The commonly used fuel in these engines is heavy fuel oil (HFO) which contains sulphur as impurity. This leads to the formation of the sulfur oxides ( $\text{SO}_x$ ) and sulfuric acid ( $\text{H}_2\text{SO}_4$ ) [1]. High thermal efficiency of natural gas (NG) as well as lower emissions, especially  $\text{SO}_x$  and particulate matter (PM), and lower greenhouse gas (GHG), makes the NG to be a promising alternative fuel to solve the emission problems of marine engines. There are two kinds of NG-diesel dual-fuel marine engines based on their ignition principles. These engines can be categorized as the premixed lean burn combustion engines and the high pressure direct injection (HPDI) NG engines [2]. In HPDI-NG engines, a small amount of pilot fuel and natural gas are directly injected into the cylinder near top dead center (TDC). The combustion process of the injected NG is initiated by the pilot fuel ignition. Therefore, the pilot

diesel injection plays a critical role in this kind of engines [3].

Many researches have been carried out the HPDI NG-diesel dual-fuel engines. In ref. [4], HPDI two-stroke NG-diesel engine tests were performed at different loads with a pilot diesel fuel below 5% of the total fuel amount. The  $\text{CO}_2$  and  $\text{NO}_x$  were improved by around 20% and 23%, respectively compared to conventional diesel engine. The exhaust soot emissions were found to be negligible compared to that in a conventional diesel engine [4]. Lucchini et al. [5] used the tabulated kinetics method to simulate the combustion in a HPDI NG-diesel dual-fuel marine engine in their CFD study. They concluded that using two separated tables for diesel and NG is accurate when two distinct jets of diesel and NG are directly injected inside the cylinder where only the air is present. However, using two separated tables is not recommended when diesel fuel is injected into a premixed air-NG mixture. In a recent study, Hult et al [6] conducted an experimental study on the dual-fuel MAN 4T50ME-X test engine. They compared the flames of dual-fuel and a diesel engine and concluded that the flame length development is similar for two flames because the gas injection system was tuned to achieve a similar combustion rate as the diesel engine mode. However, the lift-off length (which is defined in [6] as the smallest distance from injector to where soot starts form) for the gas flame has a higher value than diesel.

The aforementioned studies did not focus on the effects of the injection direction of the pilot fuel on the combustion characteristics and emissions of the two-stroke HPDI dual-fuel marine engine. Due to the importance of the pilot fuel, the direction of this fuel is varied. The reminder of the paper is presented as follows. In the next section, the test engine specifications

used in experimental test is presented. It is followed by the description of the utilized numerical methods. In the results section, initially, the model is validated with experimental data. Finally, the flame penetration, heat transfer to walls and emissions are compared for different injection directions of pilot fuel. Conclusions from this study are outlined in the last section

## 2. ENGINE SPECIFICATIONS

CFD simulations are carried out on a two-stroke 4T50ME-X optical test engine located at MAN Energy Solutions, Denmark. Details of the engine specifications are presented in Table 1. The simulated engine is equipped with one diesel injector and one gas injector, where each injector has four nozzle holes.

Table 1 Dual-fuel MAN 4T50ME-X test engine specifications

Bore	500 mm
Stroke	2200 mm
Connecting rod	2885 mm
Engine load	75%
Engine speed	122 rpm
Diesel start of injection	179.5 CAD ABDC
Gas start of injection	180.5 CAD ABDC

## 3. NUMERICAL MODELING

3-D CFD simulations are performed using the CFD software STARCCM+ version 14.06.012-R8. The turbulent flow is modeled using the Unsteady Reynolds Averaged Navier Stokes (URANS) method with the  $k-\omega$  Shear Stress Transport (SST) model [7]. For diesel spray, Rosin Rammler is utilized to model the initial droplet size distribution, while Reitz-Diwakar model is applied to simulate the secondary breakup. In this study, the ignition and combustion processes of the pilot diesel fuel are simulated using a n-heptane model while the liquid properties of the diesel fuel are represented by tetradecane ( $C_{14}H_{30}$ ) due to the similarity of thermo-physical properties of  $C_{14}H_{30}$  with diesel fuel [1]. NG is represented by the methane fuel as the main component of natural gas. The Seidel mechanism with 56 species and 128 reactions is used to simulate the dual fuel combustion of diesel and methane in this study [9]. The experimental mass flow rate is used for both diesel and gas injections. To consider the effects of the scavenging flow effects on the combustion a tangential velocity with solid body rotation profile is initiated at 120 crank angle degree (CAD) after bottom dead center (ABDC), which is also the start of simulation. The initial axial velocity is set

using a linear velocity profile, starting from zero in the vicinity of the exhaust valve and increasing to be the same value as the piston velocity near the piston [8].

As it is mentioned in the introduction section, the pilot diesel fuel plays an important role as the trigger of the combustion in the HPDI dual fuel marine engine and has an important role in the combustion. Therefore, the interaction between the pilot diesel spray and gas spray may have a significant effect on the combustion. In the 4T50ME-X test engine, two separate injectors for diesel and natural gas located inside the cylinder and each injector has four nozzle holes. The direction of the injections for the base case is presented in Figure 1. Half of the cover surface is removed to better illustrate the injectors. The diesel pilot fuel injector is rotated around the Z-axis (which is illustrated in Figure 1) related to the

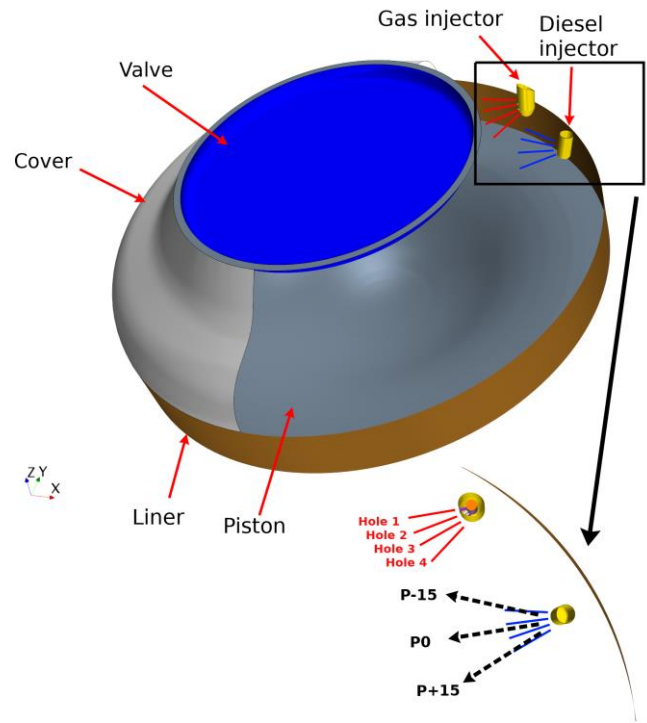


Fig 1 The injection direction for diesel and gas fuels.

initial direction. The pilot fuel is rotated 15 deg clockwise (P-15) and 15 deg counterclockwise (P+15), while the base case using the reference spray axis is named as P0.

## 4. RESULTS AND DISCUSSION

### 4.1 Validation

For validation of the numerical model, the in-cylinder pressure and heat release rate (HRR) is compared with the experimental data based on CAD ABDC in Figure 2. A

reasonable agreement between the CFD results and measurements. The error in the prediction of compression pressure and maximum pressure are around 0.2% and 0.6%, respectively.

#### 4.2 Parametric study and discussion

The in-cylinder pressure and the heat release rates are compared for the three different injection directions in Figure 3. As it can be seen, all the first peaks of the heat release rate which belong to the pilot diesel fuel

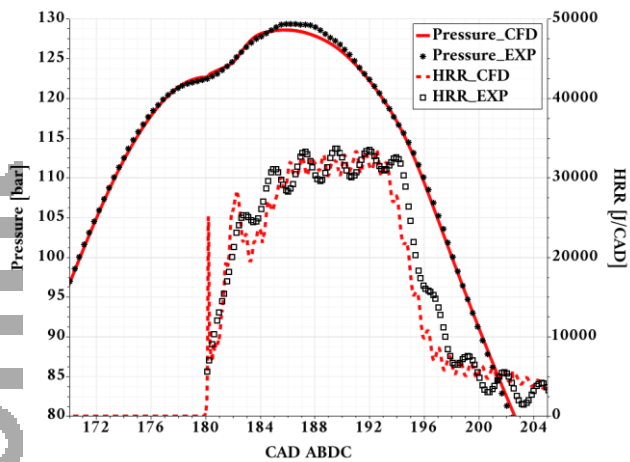


Fig 2 Comparison of measured and calculated in-cylinder pressure and heat release rate (HRR).

combustion are quite similar for all cases. However, the change in the injection direction of the pilot fuel changes NG combustion timing and intensity considerably, which is observable by comparison of the second increase in the HRR plot. The maximum pressure and HRR for the P+15 case is higher than others which will be elaborated more in this section.

Figure 4 illustrates the shape of flame and interaction between diesel and gas jets for various injection directions of the pilot fuel at different CADs on a plane section which is placed at a height where it intersects the middle of the first gas nozzle hole (Hole 1). As it can be seen, the pilot diesel flame comes in contact with the gas spray at around 181 CAD ABDC for the P-15 case, while there is no interaction between pilot injection and gas injection for the P0 and P+15 cases. For the P0 case, the pilot fuel interacts with the gas spray around 182 CAD ABDC which can also be observed in the heat release rate plot at 182 CAD ABDC cf. Figure 3. For the P+15 case, the interaction between the pilot flame and gas spray is postponed until 184 CAD ABDC. It is worth mentioning that for the P+15 case, a bigger cloud of the

NG is accumulated inside the combustion chamber before it starts to burn. By comparing the flame contour at 184 and 185 CADs ABDC for the P+15 case, it is observed that a larger amount of methane gas is burned, which is the main reason for large values of the heat release rate for the P+15 case. This will be elaborated more in next Figures (please see Figure 7).

As depicted in Figure 4, the flame characteristics and sizes vary for different injection directions of the pilot fuel. This is expected to lead to different amount of flame quenching on the combustion chamber walls. Therefore,

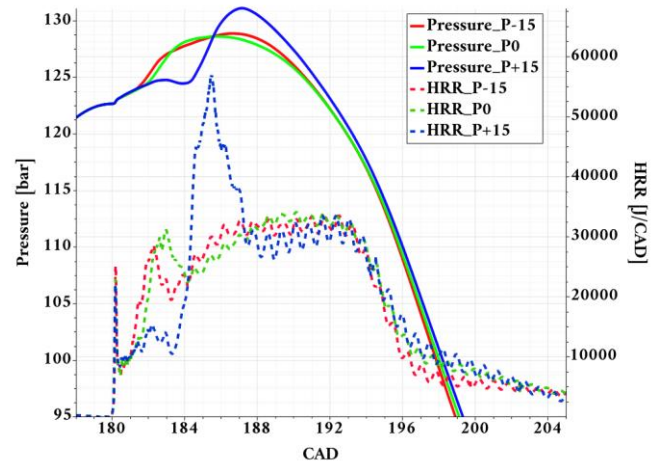


Fig 3 Comparison of in-cylinder pressure and heat release rate for various injection directions of the pilot fuel.

the heat transfer for four different wall regions of the combustion chamber is next investigated. These regions include cover, valve, piston, and liner cf. Figure 1.

The heat transfer to these walls is compared for different injection directions of the pilot fuel to give additional information about the location and penetration of flame inside the combustion chamber. As it can be seen in Figure 5, the heat transfer to the liner increases in the P-15 case. This is because the flame gets closer to the liner as it can be seen in Figure 4 as well. Furthermore, the NG fuel combustion timing can be interpreted from the liner heat transfer plot which shows the gas combustion for the P+15 case delayed around 3-4 CADs in comparison with the P-15 case. The heat transfer to the cover is presented in Figure 5. The amount of the heat transfer to the cover for the P-15 case is higher than others. The heat transfer to the cover for the P+15 case is lower than P0 case before 193 CAD ABDC and after this CAD, this heat transfer is higher for the P+15. This is because of the combustion of the big cloud of NG in the vicinity of cover for the P+15 case which leads to a higher temperature and a higher heat transfer

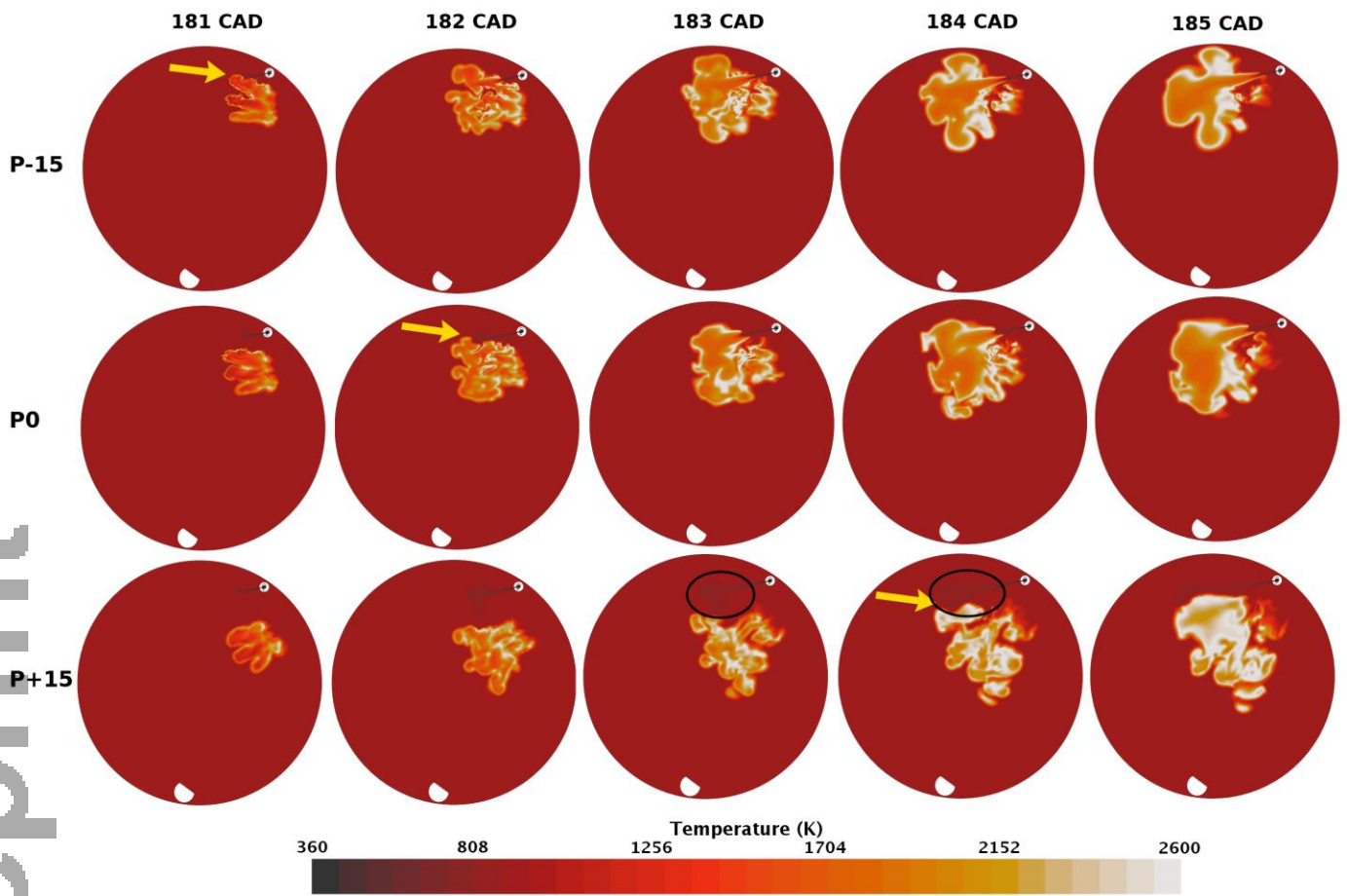


Fig 4 Contour of temperature at different CADs ABDC for various injection directions of the pilot fuel.

to cover for this case than that of P0 case after 193 CAD ABDC. The heat transfer to the valve shows an interesting trend by changing the injection direction of the pilot fuel. For the P-15 case, the heat transfer to valve has the lowest value which clarifies that the flame penetrates

mostly far from the valve position. However, the P+15 case has the highest heat transfer to valve. This may be due to the pilot diesel fuel which is mostly injected to the inner position of cylinder close to the center where swirl has its lowest value in this region and, the flame is not

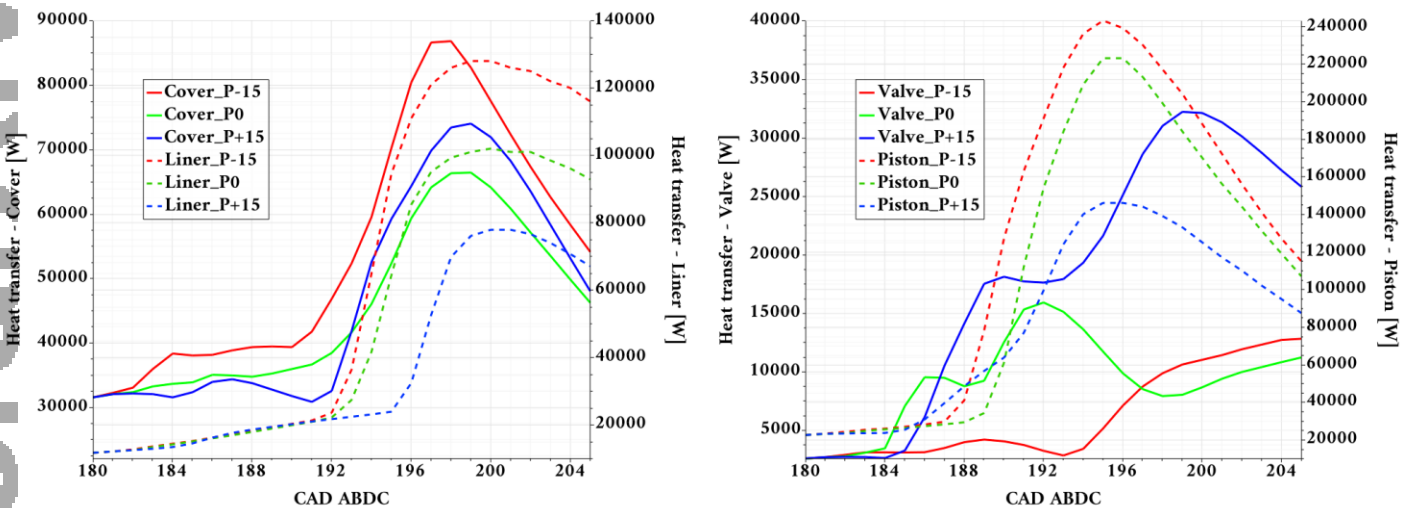


Fig 5 Heat transfer to different surfaces of the combustion chamber for various injection directions of the pilot fuel.



directed by the gas spray and swirl inside the cylinder and penetrates until it reaches to the valve surface. However, for the P-15 case, the pilot fuel is injected to

injection (holes 1 and 2 as depicted in Figure 1) reaches the piston later which leads to lower heat transfer to the piston in comparison with P0 and P-15 cases. Based on these findings it can be concluded that the flame for the P-15 case impinges onto the liner and cover, while the flame for the P+15 case, flame impingement mainly occurs at the valve. The total heat transfer to the combustion chamber is illustrated in Figure 6, shows that the heat loss for the P+15 case is lower than other cases.

The mass averaged value of NOx and methane mass fraction is presented in Figure 7. As it can be seen the value of NOx for the P+15 case is higher than other cases after 185 CAD ABDC. It is also obvious that large amount of unburned methane is accumulated inside the combustion chamber for the P+15. This large cloud of methane starts to combust around 184 CAD ABDC which leads to high temperature regions and higher values of NOx formation for the P+15 case. It is also worth mentioning the unburned methane value is slightly higher for the P+15 case than the other cases.

The mass averaged value of CO inside the combustion chamber is presented in Figure 8. The CO mass fraction for the P-15 case is higher than others because of the higher interaction of the flame with cold walls which leads to higher values of CO inside the combustion chamber.

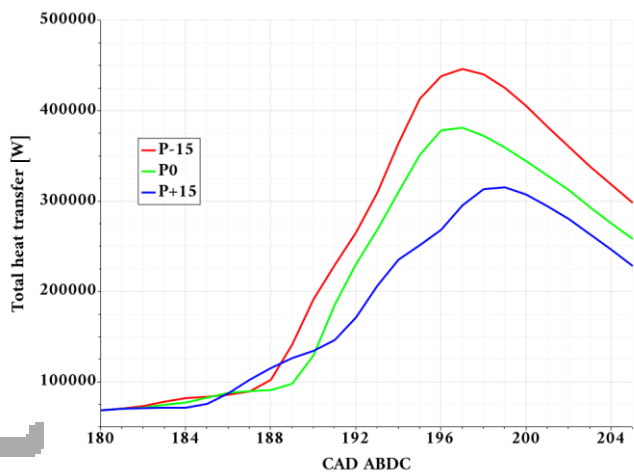


Fig 6 Total heat transfer to combustion chamber for various directions of the pilot fuel injection.

the high swirl region and on the other hand it directly injected inside the high velocity gas spray which pushes the diesel flame toward the liner and cover.

Heat transfer to piston is presented in Figure 5 for different injection directions of the pilot fuel. It can be

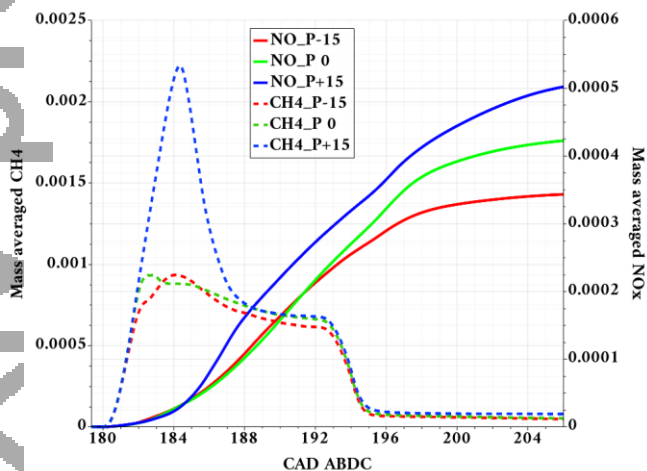


Fig 7 Mass averaged value of NOx and CH4 mass fraction for different injection directions of the pilot fuel.

seen that the heat transfer to the piston is lower for the P+15 case. There are four different nozzle holes for gas injector cf. Figure 1. When the pilot fuel is injected far from the gas spray (P+15), the gas flow through the holes close to the pilot flame starts to burn before than the others. Therefore, the flame of the holes far from pilot

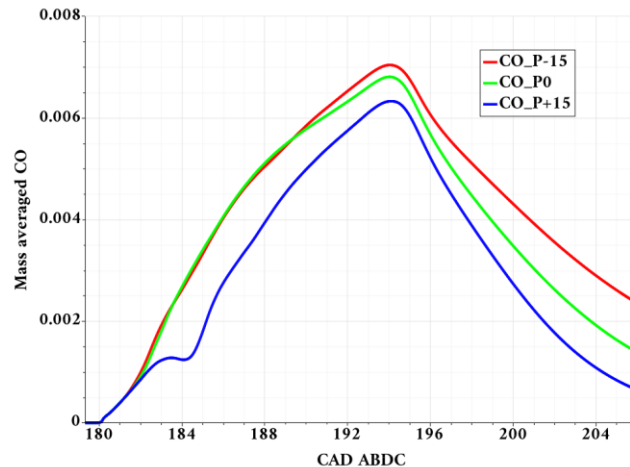


Fig 8 Mass averaged value of CO mass fraction for different injection directions of the pilot fuel.

#### 4.3 Conclusions

The combustion, emissions and flame propagation of a dual-fuel two-stroke marine engine is studied by variation of the injection direction of the pilot fuel. It is found that by injecting the pilot fuel to the inner region

of the cylinder (P+15), NG combustion is delayed due to the late interaction between the pilot flame and gas spray. This leads to intense combustion of a large cloud of the NG and higher maximum values of in-cylinder pressure and HRR. The heat transfer analysis clarified that for the P+15 case, flame mostly impinges onto the valve, while P-15 flame has higher impingement on the cover and liner as well as piston surface. The P+15 case has the lowest heat loss while the higher NO<sub>x</sub> emission belongs to this case as well as higher unburned methane. On the other hand, the highest value of CO emission is observed for the P-15 case. Therefore, considering the similar pressure curve for the P-15 and P0, the P-15 case is not recommended. The results of this study clarified that the direction of the injection of the pilot fuel is an important parameter for the surface heat transfer and production of harmful exhaust gasses.

#### ACKNOWLEDGEMENT

The authors gratefully acknowledge the financial support from the Independent Research Fund Denmark (DRF) and MAN Energy Solutions under the grant number 8022-00143B. The authors also would like to thank MAN Energy Solutions, Denmark for sharing the experimental data. The computation was performed using the Niflheim cluster at the Technical University of Denmark (DTU).

#### REFERENCE

- [1] Pang, K. M., Karvounis, N., Walther, J. H., & Schramm, J. (2016). Numerical investigation of soot formation and oxidation processes under large two-stroke marine diesel engine-like conditions using integrated CFD-chemical kinetics. *Applied Energy*, 169, 874-887.
- [2] Yang, R., Theotokatos, G., & Vassalos, D. (2020). Parametric investigation of a large two-stroke marine high-pressure direct injection engine by using computational fluid dynamics method. *Proceedings of the Institution of Mechanical Engineers, Part M: Journal of Engineering for the Maritime Environment*, 1475090219895639.
- [3] Ishibashi, R., & Tsuru, D. (2017). An optical investigation of combustion process of a direct high-pressure injection of natural gas. *Journal of Marine Science and Technology*, 22(3), 447-458.
- [4] Juliussen, L. (2011). MAN B&W ME-GI engines Recent research & results. ISME KOBE 2011.
- [5] Lucchini, T., Della Torre, A., D'Errico, G., & Onorati, A. (2019). Modeling advanced combustion modes in compression ignition engines with tabulated kinetics. *Applied energy*, 247, 537-548.
- [6] Hult, J., Matamis, A., Baudoin, E., Mayer, S., & Richter, M. (2020). Optical Characterization of the Combustion Process inside a Large-Bore Dual-Fuel Two-Stroke Marine Engine by Using Multiple High-Speed Cameras (No. 2020-01-0788). SAE Technical Paper.
- [7] Wilcox, D. C. (2008). Formulation of the kw turbulence model revisited. *AIAA journal*, 46(11), 2823-2838.
- [8] Nematy, A., Ong, J. C., Jensen, M. V., Pang, K. M., Mayer, S., & Walther, J. H. (2020). Numerical study of the scavenging process in a large two-stroke marine engine using URANS and LES turbulence models (No. 2020-01-2012). SAE Technical Paper.
- [9] Seidel, L., Netzer, C., Hilbig, M., Mauss, F., Klauer, C., Pasternak, M., & Matrisciano, A. (2017). Systematic reduction of detailed chemical reaction mechanisms for engine applications. *Journal of Engineering for Gas Turbines and Power*, 139(9).